ISSN 2447-6102

Article

ANALYSIS OF PROPELLANT INJECTION IN A LOW-POWER ELECTRODELESS THRUSTER FOR CUBESATS

Silvano, H.E. [1,*], Cerda, R.A.M.[1,2] , Costa, S.G.S.P. [2] Almeida, J.C.M [2] and Ferreira, J.L. [2]

[1] Faculty of Science and Technology in Engineering, University of Brasilia, Brasilia-DF, Brazil; e-mail@e-mail.com

[2] Plasma Physics Laboratory, Institute of Physics, University of Brasilia, Brasilia-DF, Brazil; e-mail@e-mail.com

***** Correspondence: helenaemerys@gmail.com

Received: Outubro/2025; Accepted: Novembro/2025; Published: Novembro/2025

Abstract: Miniaturized satellites, particularly CubeSats, have revolutionized access to space by enabling low-cost scientific and technological missions. However, their operational capabilities are strongly limited by the lack of efficient, compact propulsion systems. In this context, electrodeless plasma thrusters, such as low-power helicon devices, emerge as promising alternatives due to their simplicity, robustness, and scalability. This work investigates the effect of propellant injection configuration on the performance of a low-power electrodeless thruster designed for CubeSats. Numerical simulations were carried out using the Molecular Flow Module of COMSOL Multiphysics to analyze the neutral gas distribution in two propellant injection modes: normal and vortex. The results reveal that the vortex mode significantly enhances the neutral gas density inside the discharge chamber, achieving a 43% increase compared to the normal mode. This improvement is attributed to the radial injection geometry and longer gas residence time, which increases the probability of ionization events. The neutral density profiles obtained from the simulations were fitted with a fourth-degree polynomial function and subsequently implemented as input for particle-in-cell (PIC) simulations, allowing for a self-consistent analysis of plasma behavior under realistic neutral distributions. The findings highlight the critical role of injection configuration in improving thruster efficiency and demonstrate that optimizing propellant injection is a cost-effective strategy for enhancing electrodeless plasma propulsion systems for CubeSats and other miniaturized spacecraft operating under severe power, mass, and volume constraints.

Keywords: electric propulsion; numerical simulation; CubeSats; molecular flux density; electrodeless thruster.

1. Introduction

In recent years, the use of miniaturized satellites, particularly CubeSats, has grown considerably. This technology holds the potential to revolutionize the space industry by enabling individual countries, regional governments, and small companies to establish their own space missions. The economic advantages of small satellites drive their growing adoption, with the development of propulsion systems being crucial for enhancing CubeSat capabilities. Complex missions demand precise orbit control and maintenance, necessitating specialized propulsion systems. Additionally, concerns over space debris have led to stringent regulations that emphasize the necessity for efficient propulsion systems.

Electric propulsion refers to devices that employ electricity to accelerate a propellant, and its concept dates to the early 20th century, with pioneering contributions from Robert Goddard, Tsiolkovskiy, and Hermann Oberth, followed by significant developments in the United States and the Soviet Union. Since 2004, the Plasma Physics Laboratory of the University of Brasília (LFP-UnB) has been developing electric propulsion devices, including Hall-type thrusters with permanent magnets, which reduce power requirements for operation.

Integrating propulsion systems into CubeSats presents significant challenges due to strict limitations on mass, volume, power, and cost. Traditional Hall thrusters, for instance, can achieve higher thrust levels compared to ion thrusters but face difficulties when scaled down to micro and nanosatellite sizes. Increased surface-to-volume ratios

lead to enhanced wall collisions, heating, and erosion, as well as challenges in maintaining the magnetic circuit. These limitations have motivated the development of alternative electric propulsion concepts better suited for low-power regimes.

The helicon plasma thruster (HPT) has emerged as an attractive option due to its simplicity, absence of electrodes, and scalability. It uses electromagnetic radiofrequency (RF) waves to ionize and accelerate the plasma, providing high reliability and durability. A low-power variant of the HPT, known as the ambipolar thruster, was developed as part of the miniaturization trend in the aerospace industry. This device operates at lower power levels while maintaining efficient plasma production and confinement, making it ideal for CubeSat applications.

The ambipolar thruster consists of a discharge chamber surrounded by a radiofrequency antenna responsible for plasma generation, and two rings of permanent magnets that provide magnetic confinement. The main components of the ambipolar thruster are shown in Figure 1. . Neutral gas is injected into the chamber through distributor holes that ensure homogeneous gas distribution. The magnetic field lines are oriented primarily along the axial direction, and the magnetic strength near the physical nozzle is weaker, creating a magnetic nozzle configuration that directs the plasma outward. Because electrons have a much smaller mass than ions, they are expelled first, establishing an electric field that accelerates ions and generates thrust. The use of permanent magnets helps minimize power consumption, an essential feature for small satellites with limited onboard energy.

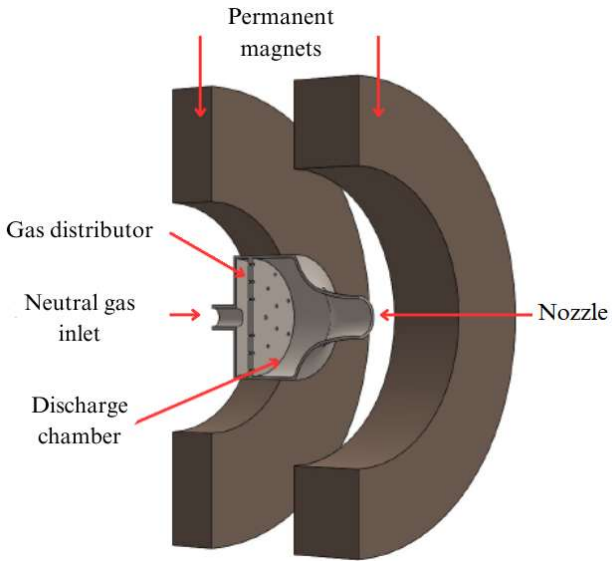

Figure 1. Schematic diagram of the low-power helicon (ambipolar) thruster, showing its main components: permanent magnets, discharge chamber, physical nozzle, neutral gas inlet, and gas distributor plate with injection holes. The helicon antenna, described in the text, is not shown in this figure.

The operational parameters of plasma thrusters—such as thrust, specific impulse, and efficiency—can be predicted via numerical simulations. Models like the particle-in-cell (PIC) method, coupled with Monte Carlo collision (MCC) techniques, accurately describe plasma dynamics in the presence of electromagnetic fields and neutral gases. Since the neutral gas distribution in the ionization chamber directly affects thruster performance, an accurate description of its density profile is essential.

The objective of this work is to analyze the neutral gas behavior in a low-power ambipolar thruster through numerical simulations. The neutral gas density profile is fitted to a polynomial function, which can be used as an input for plasma simulation codes implementing the PIC-MCC method.

2. Materials and Methods

Numerical simulations of the neutral gas density inside the discharge chamber were performed using the Molecular Flow Module of the COMSOL Multiphysics software. Two configurations were analyzed for the distributor holes: the *normal mode*, where the holes are aligned with the normal of the injection plate, and the *vortex mode*, where the holes are tilted, producing a circulation vortex within the chamber.

2.1. COMSOL

The neutral gas density data used in this work were obtained using the molecular flow model of the COMSOL Multiphysics software, which is a finite element simulation software widely utilized across various physical and engineering domains, particularly in scenarios involving coupled and Multiphysics phenomena. The molecular flow module stands out for its capability to simulate free molecular flows within intricate geometries.

The molecular flow module computes crucial parameters such as molecular flow, pressure, and density. The core methodology employed is the angular coefficient method of interactions, a specialized variant of the radiation method tailored specifically for vacuum applications. This approach involves aggregating the incoming molecular flux to a surface element with the outflow from all other visible areas.

The molecular density n at a surface is obtained by:

$$n = J\sqrt{(\pi m/2k_B T)} \quad (1)$$

where *J* is the outgoing flux, *m* the molecular mass, *kB* Boltzmann's constant, and *T* the temperature.

In this study, the inlet conditions were: argon flow rate of 12 sccm (molecular weight 0.04 kg/mol), surface temperature of 293.15 K, and pressure of 0.00133 Pa (approximately 10^{-5} Torr).

The applicability of the molecular flow model was verIfied by computing the Knudsen number K_n, which characterizes the degree of gas rarefaction, and is defined as the ratio of the equivalent molecular free path to a representative physical length scale:

$$k_n = l/a \quad (2)$$

where l is the equivalent molecular free path, and a is the representative physical length scale. The equivalent molecular free path is given by:

$$l = (\mu v_{\mathrm{m}})/P \quad (3)$$

where v_m is the most probable molecular velocity, which can be obtained as follows:

$$v_{\mathrm{m}} = \sqrt{(2K^{\mathrm{B}}T/m)} \quad (4)$$

where P represents the gas pressure, and μ is the gaseous viscosity. The Knudsen number K_n within the simulation domain obtained is larger than 1; therefore, intermolecular collisions can be neglected, and the molecular flow model is valid.

In the normal mode, the propellant enters through a main channel, passes a pre-mixing chamber, and is injected axially into the discharge chamber through the distributor plate. The configuration in question is illustrated in Figure 2. The plate is 1 mm thick and contains 25 cylindrical holes with a radius of 0.25 mm. For the numerical domain, the gas path was modeled as two-dimensional circular inlets.

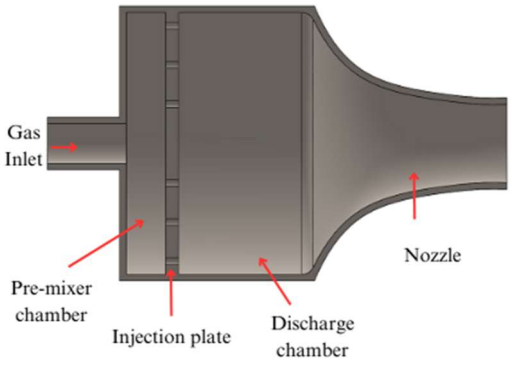

Figure 2. Side view of the low-power helicon thruster showing its main components, namely, the gas inlet, the pre-mixer chamber, the injection plate with holes, the discharge chamber, and the nozzle. The version shown here corresponds to the 'normal mode' prototype.

In the vortex mode, the gas follows the same path as in the normal configuration but is injected at an angle of 30° relative to the injector plate walls, generating a radial flow vortex inside the discharge chamber. This swirling motion increases gas residence time and density, potentially improving thruster efficiency. The inclined injection channels appear as elliptical inlets in the simulation domain, with a major radius of 0.5 mm and a minor radius of 0.25 mm. Figures 3. illustrate the thruster structure of the simulation domain used to analyze gas distribution in both modes.

(**a**) (**b**)

Figure 1. Perspective view of the simulation domain, showing the gas distributor plate in the normal mode (a), and the vortex mode (b).

2.1. Polynomial fit

The extracted density profile obtained in the previous section was processed and fitted using the MATLAB software, which is a high-performance software designed for numerical computing. It enables matrix manipulations, data visualization in graphs, algorithm implementation, and allows expressions to be written in a form that closely resembles standard mathematical notation, unlike traditional programming languages.

The neutral gas density data extracted from the COMSOL simulation that represents the distribution of neutral gas density as a function of the distance from the base of the discharge chamber, was imported into MATLAB from a .dat file containing two columns: axial position (x) and neutral density (y).

3. Results

3.1. COMSOL

Figure 4 shows a cross-section of the resulting neutral gas density for the "normal" mode, whereas Fig. 4 (b) shows the neutral density for the "vortex" mode. The cross section is defined as a surface at an axial distance of 1 mm from the injection plate. The injection holes are represented by continuous thin lines, superposed to each figure as a

reference. This figure shows that the neutral density increases around the injection holes as expected, and is highest in a region surrounding the central area of the discharge chamber. Note that the color scales are different. For the normal mode, the maximum value of the neutral density is 1.51 x 10^{21} m^{-3} whereas the vortex mode has a maximum value of 2 x 10^{21} m^{-3}. This indicates that the vortex mode results in an increase of the neutral gas density, close to the injection plate.

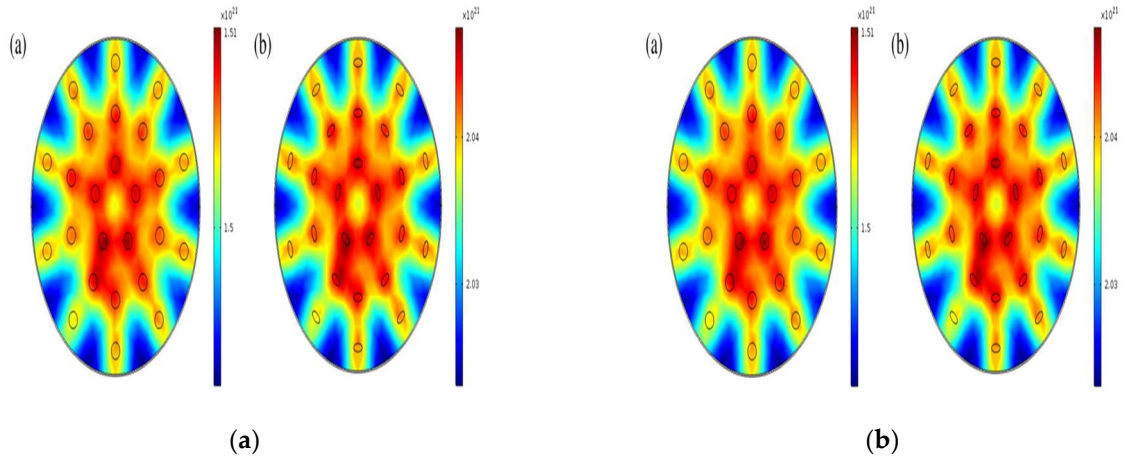

(**a**) (**b**)

Figure 4. (**a**) Descriptio Density distribution of neutral gas in a cross-section plane for (a) the normal mode, and (b) the vortex mode. Thin lines indicate the contour of the distributor holes. Color scales are indicated for each panel.

Figure 5. shows the neutral gas density as a function of the axial distance from the injection plate, obtained at the center of the discharge chamber. The normal mode is shown in dark green, while the vortex mode is shown in dark blue. Both curves display similar shapes, with a maximum value near the injection plate, and decreasing values as the distance increases. The density decreases at a faster rate at a distance around 15 mm, which is close to the physical nozzle near the exit region. From this figure it is clear that the neutral gas density of the vortex mode is higher than the normal mode for all values of the axial distance, demonstrating that the vortex mode leads to an increase of the gas density inside the discharge chamber. Close to the injection plate, the vortex mode results in a 43 % increase with respect to the normal mode, as seen, unfortunately this result can't be used directly as an input for for plasma simulation codes implementing the PIC-MCC method without a polynomial fit.

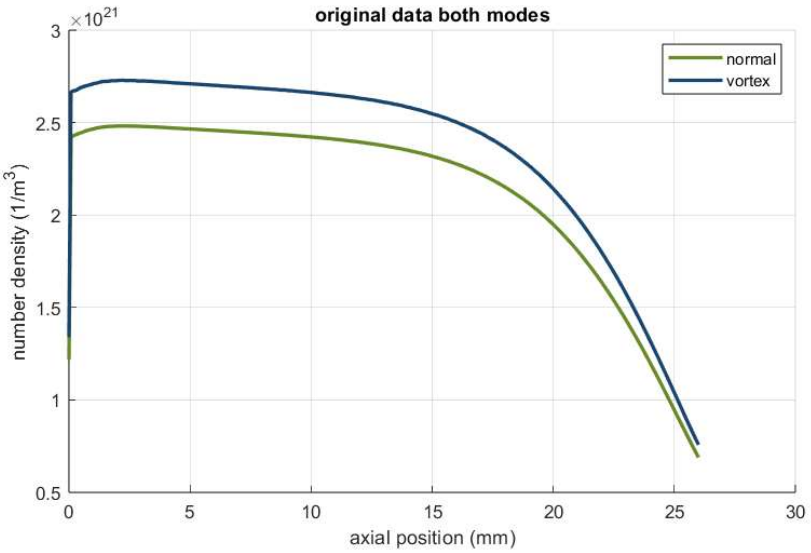

Figure 5. The neutral gas density distribution as a function of the distance (in mm) from the injection plate, computed at the center of the discharge chamber, for the normal mode (dark green line) and vortex mode (blue line).

3.1. MATLAB

A fourth-degree polynomial regression was applied using the polyfit function in MATLAB to perform the fitting, and the polyval function was used to evaluate the resulting curve over the original domain. The resulting polynomial for normal injection mode can be written as follows:

$$p_n(x) = 2.2478 \times 10^{20} - 4.2321 \times 10^{23}x - 3.3112 \times 10^{25}\,x^2 - 1.2388 \times 10^{27}x^3 - 1.8003 \times 10^{28}\,x^4 \quad (5)$$

where x represents the axial distance measured from the gas distributor.

Now, for the second injection mode — the vortex mode, with an angle of 45° — the expression takes the form:

$$p_v(x) = 2.4767 \times 10^{20} - 4.6484 \times 10^{23}\,x - 3.6326 \times 10^{25}\,x^2 - 1.3569 \times 10^{27}\,x^3 - 1.9683 \times 10^{28}\,x^4 \quad (6)$$

The polynomial degree was chosen to accurately capture the physical trend while avoiding overfitting. The quality of the fit was assessed visually by overlaying the fitted curve on the original data points, confirming the agreement between them, as shown in Figure 6 for the normal mode and Figure 7 for the vortex mode. The fitted curve deviates from the molecular flow simulation at $x \approx 0$ mm. This can be improved by increasing the degree of the fitting polynomial; however, the helicon antenna is centered at around $x \approx 10$ mm, and the maximum of the gas ionization occurs around this position. Therefore, we believe that the small deviation near $x \approx 0$ mm can be disregarded.

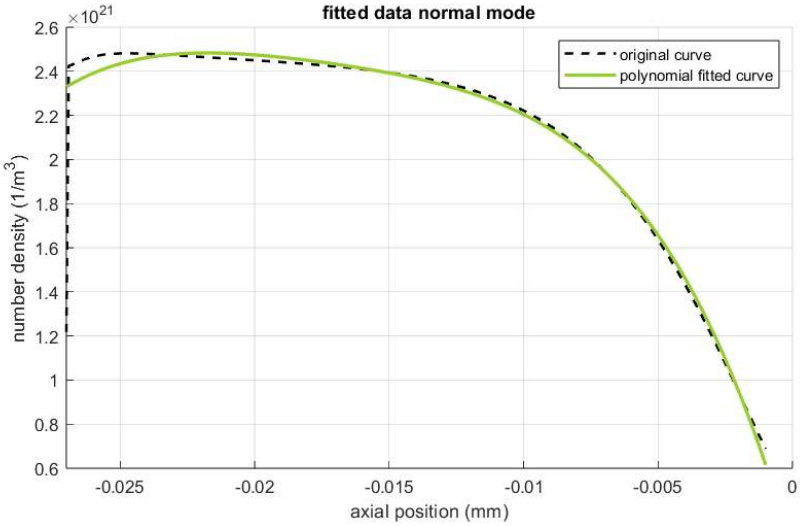

Figure 6. The neutral gas density as a function of axial distance from the gas distributor within the ionization chamber, obtained from the numerical simulation of the molecular model ("original curve", dashed black curve) and a fourth-degree polynomial fit (green curve).

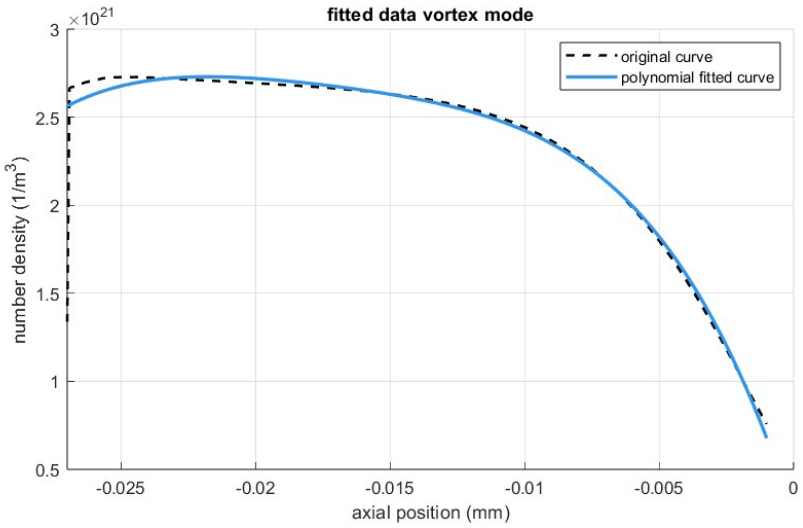

Figure 7. The neutral gas density as a function of axial distance from the gas distributor within the ionization chamber, obtained from the numerical simulation of the molecular model (“original curve”, dashed black curve) and a fourth-degree polynomial fit (blue curve).

Figure 8 compares the two curves obtained under different injection modes, each fitted with a polynomial regression.

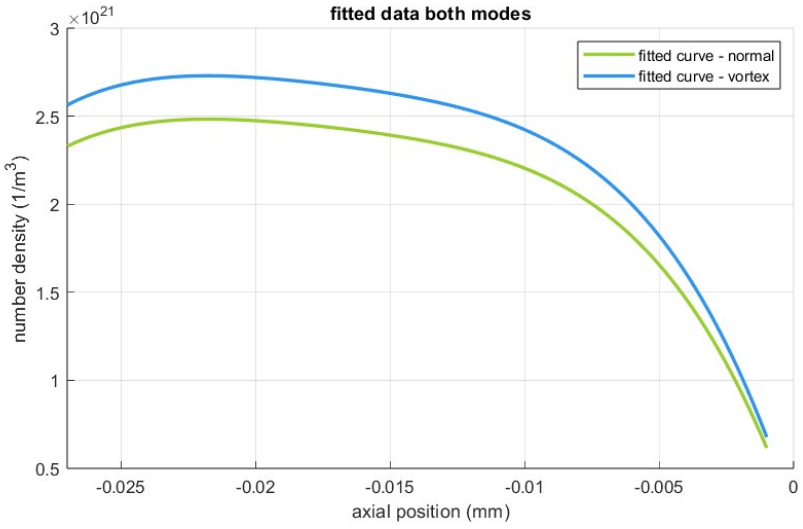

Figure 8. The neutral gas density as a function of axial distance from the gas distributor within the ionization chamber, obtained from the numerical simulation of the molecular model for two injections modes, with a fourth-degree polynomial fit ("normal mode", green curve) and ("vortex mode "blue curve).

The comparison between the two injection modes highlights a significant difference; the "vortex" mode leads to an increase of approximately 43\% in the neutral density within the discharge chamber when compared to the "normal" mode. This enhancement can be attributed to the radial component of the injected flow and the resulting longer residence time of the propellant molecules. From a physical standpoint, this higher density implies a greater availability of neutrals for electron–neutral collisions, which in turn favors more efficient ionization and potentially increases the overall thruster performance.

Nevertheless, the present results are based on molecular flow modeling alone, which does not include plasma feedback effects, although the relative comparison between injection modes remains robust. The resulting polynomial

will serve as an input to subsequent simulations involving plasma particle dynamics. Figure 9 shows a preliminary result of an axial-radial two-dimensional particle-in-cell simulation, using the software OOPIC. The neutral density has been set to the “vortex” case, implementing the corresponding polynomial in the configuration file of OOPIC. In the Figure 9 the blue rectangles represent the walls of the ionization chamber, and blue dots represent argon ions. From this figure it is clear that a high density of particles occurs inside the ionization chamber, and decreases towards the thruster exit, as expected from the 4-th degree polynomial given by Equation 6.

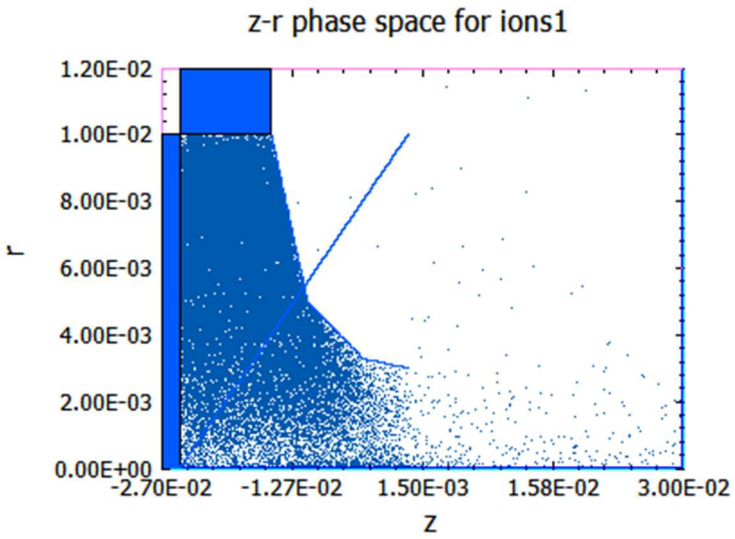

Figure 9. The z-r phase space for ions inside the ionization chamber. The blue rectangles represent the walls of the ionization chamber, and blue dots represent argon ions.

4. Discussion

This work presented results of numerical simulations of a molecular model of a neutral gas in the ionization chamber of a low-power helicon plasma thruster. Two modes were simulated, namely, the normal'' mode, in which the holes in the gas distributor wall are aligned to the wall surface normal, and the vortex'' mode, in which the holes form an angle of 45 degrees with the wall surface normal. The results of the molecular model show that the neutral gas density increases in the “vortex” mode compared to the “normal” mode, thereby improving thrust and efficiency.

A fourth-degree polynomial was computed by applying a nonlinear fitting to the profiles obtained from the molecular model. These polynomials can be implemented directly as inputs to the PIC codes, enabling a more seamless integration between neutral flow modeling and plasma kinetic simulations. A representative result from a numerical simulation using the XOOPIC code was shown, while extended simulations are currently in progress at the Laboratory for Simulation of Plasma Propulsion at the University of Brasília.

Overall, this study demonstrates that propellant injection configuration plays a key role in the efficiency of low-power electrodeless plasma thrusters. The vortex injection scheme emerges as a promising solution to increase the neutral density available for ionization, representing a significant step toward the optimization of propulsion technologies for CubeSats and other miniaturized satellites, where strict limitations on power, mass, and volume constrain propulsion system design. In this context, optimizing propellant injection emerges as a cost-effective strategy to enhance thruster performance without major modifications to the system architecture.

Funding: This research was funded by FAPDF, grant number 383

Acknowledgments: HES acknowledges support from FAPDF, Brazil (grant 383/2023). RAM acknowledges support from CNPq, Brazil (grants 407341/2022-6, 407493/2022-0), FAPDF, Brazil (grant 383/2023) and the Brazilian Space Agency (TED 000529/2024). SGSPC acknowledges support from CNPq (grant 407341/2022-6). JCMA acknowledges support from CNPq (grant 407493/2022-0). JLF acknowledges support from CNPq (grant 405907/2022-2) and the Brazilian Space Agency (TED 000529/2024). All numerical simulations were performed using computational resources at the Laboratory for Simulation of Plasma and Electric Propulsion (LaSPPE) at the Institute of Physics, UnB.

Conflicts of Interest: The authors declare no conflict of interest.

References

1. Heidt, H.; Puig-Suari, J.; Moore, A.; Nakasuka, S.; Twiggs, R. CubeSat: A new generation of picosatellite for education and industry low-cost space experimentation. Proceedings of the 14th Annual AIAA/USU Conference on Small Satellites, 2000.
2. Manente, M.; Trezzolani, F.; Magarotto, M.; Fantino, E.; Selmo, A.; Bellomo, N.; Toson, E.; Pavarin, D. Regulus: A propulsion platform to boost small satellite missions. Acta Astronaut. 2019, 157, 241–249. https://doi.org/10.1016/j.actaastro.2018.03.043
3. Goebel, D.M.; Katz, I.; Mikellides, I.G. Fundamentals of Electric Propulsion; John Wiley & Sons: Hoboken, NJ, USA, 2023.
4. Ferreira, J.L.; Martins, A.A.; Miranda, R.; Schelin, A.B.; de Souza Alves, L.; Costa, E.G.; Coelho, H.O.; Serra, A.C.; Nathan, F. Permanent magnet Hall thruster development for future Brazilian space missions. Comput. Appl. Math. 2016, 35, 711–726. https://doi.org/10.1007/s40314-015-0249-0
5. Beal, B.E.; Gallimore, A.D.; Hargus, W.A. Plasma properties downstream of a low-power Hall thruster. Phys. Plasmas 2005, 12, 123502. https://doi.org/10.1063/1.2139308
6. Ding, Y.; Yu, D.; Jia, D.; Yan, G.; Li, H. Scaling design and experimental study on Hall thrusters with curved magnetic field. Contrib. Plasma Phys. 2011, 51(1), 68–82. https://doi.org/10.1002/ctpp.201000032
7. Raitses, Y.; Fisch, N. Parametric investigations of a nonconventional Hall thruster. Phys. Plasmas 2001, 8(5), 2579–2586. https://doi.org/10.1063/1.1369659
8. Ding, Y.; Jia, B.; Xu, Y.; Wei, L.; Su, H.; Li, P.; Sun, H.; Peng, W.; Cao, Y.; Yu, D. Effect of vortex inlet mode on low-power cylindrical Hall thruster. Phys. Plasmas 2017, 24(8), 083511. https://doi.org/10.1063/1.4995635
9. Magarotto, M.; Manente, M.; Trezzolani, F.; Pavarin, D. Numerical model of a helicon plasma thruster. IEEE Trans. Plasma Sci. 2020, 48(4), 835–844. https://doi.org/10.1109/TPS.2020.2965623
10. Sheehan, J.; Longmier, B.W.; Reese, I.; Collard, T. New low-power plasma thruster for nanosatellites. In Proceedings of the 50th AIAA/ASME/SAE/ASEE Joint Propulsion Conference, Cleveland, OH, USA, 28–30 July 2014; p. 3914. https://doi.org/10.2514/6.2014-3914
11. COMSOL. Introduction to the Molecular Flow Module. Available online: https://doc.comsol.com/5.4/doc/com.comsol.help.molec/IntroductionToMolecularFlowModule.pdf (accessed on 31 October 2025).
12. Birdsall, C.K.; Langdon, A.B. Plasma Physics via Computer Simulation; CRC Press: London, UK, 2004.
13. Bruhwiler, D.L.; Giacone, R.E.; Cary, J.R.; Verboncoeur, J.P.; Mardahl, P.; Esarey, E.; Leemans, W.; Shadwick, B. Particle-in-cell simulations of plasma accelerators and electron-neutral collisions. Phys. Rev. ST Accel. Beams 2001, 4(10), 101302. https://doi.org/10.1103/PhysRevSTAB.4.101302
14. MATLAB. Version 7.10.0 (R2010a); The MathWorks Inc.: Natick, MA, USA, 2010.
15. Verboncoeur, J. OOPIC: Object Oriented Particle-in-Cell Code. In Proceedings of the International Conference on Plasma Science (Papers in Summary Form Only Received), Madison, WI, USA, 5–7 June 1995; p. 244.